Chemical Engineering Journal 106 (2005) 119–131

Chemical Engineering Journal

www.elsevier.com/locate/cej

Conceptual design of a reactive distillation process for ultra-low sulfur diesel production

Tomás Viveros-García, J. Alberto Ochoa-Tapia, Ricardo Lobo-Oehmichen, J. Antonio de los Reyes-Heredia, Eduardo S. Pérez-Cisneros*

Departamento de Ingeniería de Procesos e Hidráulica, Universidad Autónoma Metropolitana-Iztapalapa, San Rafael Atlixco 186, C.P. 09340, México, D.F., Mexico

Received 12 July 2004; received in revised form 15 November 2004; accepted 17 November 2004

Abstract

Based on a thermodynamic analysis in terms of reaction-separation feasibility, a conceptual design of a reactive distillation column for ultra-low sulfur diesel production has been developed. The thermodynamic analysis considers the computation of reactive and non-reactive residue curve maps for a mixture that models the sulfured diesel fuel. The visualization of the reactive residue curves is posed in terms of elements. From the reactive residue curve maps, it is found that there is a high temperature region where the vaporization of hydrogen sulfide favors the elimination of the heavier organo-sulfur compounds. Considering the differences in volatility and reactivity of the organo-sulfur compounds and the phase behavior through the residue curve maps, a conceptual reactive distillation column design was developed. The reactive distillation column considers two reactive zones: In reactive zone I, located above the hydrocarbon feed stream, thiophene and benzothiophene are preferentially eliminated. In reactive zone II, located below the feed stream, dibenzothiophene and 4,6-dimethyl-dibenzothiophene (4,6-DMDBT) are mostly consumed. To validate the conceptual design, rigorous steady state simulations were performed. The design goal was stated to produce 4000 bbl/day of ultra-low sulfur diesel with a 99% conversion of 4,6-DMDBT. It is shown that reactive distillation may be considered a viable technological alternative for deep HDS of diesel.

Keywords: Ultra-low sulfur diesel; Reactive distillation; Reactive residue curves

1. Introduction

The worldwide regulations of diesel fuel are increasing the pressure on the oil industry. The European Union agreed that the maximum permissible sulfur content of diesel would be 350 wppm from the year 2000, and 50 wppm from the year 2005. This mandatory reduction is promoting changes in the oil refineries in terms of modifying the catalyst used and/or in the technology involved in the hydrodesulfurization (HDS) process. That is, higher activity of the commercial catalyst, and structural changes in the reactor configuration to increase the sulfur-compounds conversion, are needed. Specifically, the diesel produced in Mexican refineries contains around 500 wppm of sulfur and it is thought that the reduction to 50 wppm will require a very important economical investment [15]. Therefore, the study and analysis of the different technological alternatives are considered to be of high priority.

In conventional HDS process [12] several types of commercial catalytic reactors (fixed-bed, moving-bed, LC-fining, etc.) are used and they operate under similar principles. However, the fixed-bed reactor is preferred to process light feeds, while the moving-bed reactor is selected for heavy feeds hydroprocessing. The catalysts are chosen depending on the feed properties and usually include supported molybdate and tungstate catalysts promoted by either Ni or Co. γ-Alumina, zeolites, silica and silica aluminates are the typical supports.

* Corresponding author. Tel.: +52 55 58 04 46 44; fax: +52 55 58 04 49 00.
E-mail address: espc@xanum.uam.mx (E.S. Pérez-Cisneros).

1385-8947/$ – see front matter © 2004 Elsevier B.V. All rights reserved.
doi:10.1016/j.cej.2004.11.008

Nomenclature

A	element A: organic part of the organo sulfur compound
AB	molecule AB: dibenzothiophene
AC	molecule AC: biphenyl
B	element B: sulfur atom
BD	butadiene
BPH	biphenyl
BT	benzothiophene
C	element C: hydrogen molecule
CB	molecule CB: hydrogen sulfide
D	element D: *n*-hexadecane
DBT	dibenzothiophene
3-3′ DMBPH	3-3′ dimethyl-biphenyl
4,6-DMDBT	4,6-dimethyl-dibenzothiophene
Et	ethylbenzene
H	molar liquid hold-up (mol)
HDS	hydrodesulfurization
Th	thiophene
W_j	element fraction for element j
x_i	liquid mole fraction of specie i
$\overline{V}$	molar vapor flow rate (mol/h)

Knudsen et al. [18] have pointed out that there are two types of alternatives to achieve deep HDS of diesel: (1) increasing catalyst activity, and (2) improving the performance of the reaction unit. In order to develop new catalysts for deep HDS, strong efforts are being devoted to establish relationships between the catalyst structure and the reactivity towards different molecules [36]. Recently, Argonne scientists [4] identified several new diesel fuel desulfurization catalysts with improved HDS activity and selectivity, among a fair amount of publications devoted to this topic in both open and patent literature. These researchers synthesized and tested the new catalysts at 673.2 K and 27.21 atm, and they believe that it may be possible to achieve optimal HDS processing at lower temperatures and/or pressures—even for heavy crude oils. The influence of the amount of catalyst, hydrogen partial pressure, gas/oil recycle ratio, and vapor/liquid distribution, have thoroughly been discussed by Knudsen et al. [18] and Song and Ma [33]. From these works, it is apparent that by increasing the hydrogen partial pressure and reducing the hydrogen sulfide concentration in the reaction unit would lead to increase the sulfur elimination.

Van Hasselt et al. [38] pointed out that a counter-current operation of a trickle-bed reactor leads to a higher reduction of sulfur content than the conventional co-current operation. They showed that flooding limitations (i.e., commercial flow rates) could be overcome by using finned monolith catalyst packing. However, the difficulty of counter-current designs in the case of distillate hydrotreating is vapor–liquid contacting and the prevention of hot spots within the reactor [33].

Reactive distillation has become a highly promising hybrid process for many reactive systems. The application of this combined reaction-separation process was considered useful only for reactive systems limited by chemical equilibrium and it has been applied successfully to the methyl acetate and methyl-*tert*-butyl ether (MTBE) production [2,32]. The increasing interest in reactive distillation has been accompanied by the development of various simulation algorithms related to process operation and control [1,21]. The design of reactive distillation columns (RDC) has also received some attention. Most of the existing work related to RDC design is based on the transformed composition variables proposed by Doherty's group [5,9,37,6]. An alternative to this approach is the element composition concept proposed by Pérez-Cisneros et al. [27]. The main advantage of this element composition representation is that it reduces the composition space domain and simplifies the phase equilibrium with chemical reaction (equilibrium or kinetically controlled) calculations [31]. Also, the graphical visualization of the reactive phase behavior through reactive phase diagrams and/or reactive residue curve maps, constructed in terms of these element composition variables, is simplified. Specifically, the reactive residue curve maps are highly useful tools to visualize and elucidate conceptual designs of reactive distillation processes [35]. Through reactive residue curve maps it is possible: (i) to visualize the influence of the chemical reaction on the phase behavior; (ii) to observe how far from chemical equilibrium is the reacting mixture thermal condition and (iii) to identify the presence of reactive and non-reactive azeotropes [37].

Up to now, only few papers have addressed the application of reactive distillation to the deep hydrodesulfurization of diesel. Taylor and Krishna [34] discussed the possibility to apply reactive distillation concepts to hydrodesulfurization of heavy oils. Recently, Krishna [19] showed how this technology could be used. Hidalgo-Vivas and Towler [16] presented several alternative reactive distillation flowsheets to reduce the sulfur content below 500 wppm without a significant increase in process hydrogen consumption and with energy integration. However, they did not show how to apply this technology. Similarly, CdTech Company [8] claims to have the complete development of the reactive distillation technology for ultra-low sulfur diesel production, but that information is not open to the public.

An analysis of the operating conditions to obtain ultra-low sulfur diesel in a conventional HDS process [18,38] suggests that reactive distillation could be an interesting technological alternative for deep HDS of diesel. In a reactive distillation process, the countercurrent operation is the natural operation mode and the internal flows requirement can be obtained through the catalyst packing arrangement, regulating the reflux and/or the boiling ratio, and properly placing the sulfured hydrocarbon feed. A comparison between deep

Table 1
Deep hydrodesulfurization of diesel

(a) Requirements for deep-HDS of diesel in a conventional process	(b) Operating and design options in a reactive distillation operation
Counter-current operation	The nature of the reactive distillation process offer a counter-current operation
High Residence times	Increased condensed recycle
Increased H_2 partial pressure	Fresh H_2 feeds located in appropriate places along the column
Reduced H_2S partial pressure	Elimination of H_2S through vapor side streams
Catalyst Co-Mo based: higher activity at low temperatures and it promotes the direct route of sulfur elimination.	A reactive catalytic zone could be located over the HC feed with this type of catalyst, considering the temperature profile of the column
Catalyst Ni-Mo based: higher activity at high temperatures and it promotes the hydrogenation route with high partial pressures of H_2	A reactive catalytic zone could be located below the HC feed with this type of catalyst, considering the temperature profile of the column (higher temperature at the bottom of the column)
Appropriate distribution of liquid/vapor	Selection of the appropriate plate design for the non reactive stages and the height and type of packing (i.e., monolith)

(a) Conventional process, (b) reactive distillation alternative.

HDS in a conventional reactor and the operational and design alternatives offered by a reactive distillation process are shown in Table 1. It may be noted that all the operation requirements for deep HDS in a conventional reactor could be fulfilled by a reactive distillation operation if an appropriate process design is carried out.

The application of the reactive distillation concepts to the deep HDS of diesel requires a careful analysis of the reactive system in terms of at least three items: (i) thermodynamic behavior of the reactive mixture; (ii) reaction routes and kinetic expressions; (iii) heat and mass transport phenomena. The thermodynamic analysis plays a crucial role in the application of the reactive distillation technology. The thermodynamic properties of the reacting compounds and the appropriate determination of the phase behavior are needed to determine the feasibility of the separation. The visualization of this behavior through reactive phase diagrams and/or reactive residue curve maps is required to obtain the trend of the simultaneous reaction and separation process. Correct reaction kinetics expressions are very important, since inappropriate reaction kinetics may lead to unreliable process designs. The transport phenomena analysis is, perhaps, the most complex. The transport coefficients are needed for the calculation of heat and mass transfer rates and their experimental determination is a rather hard task. Besides, in reactive distillation one deals with concentrated multi-component systems where Fick's law approach is not necessarily correct. Nevertheless, important advances on this area have been reported (Krishna and Taylor, 2000).

The objective of the present work is to develop a conceptual design of a reactive distillation process for deep HDS of diesel. The design is based on the thermodynamic analysis of the reactive system in terms of the reaction-separation feasibility. This analysis considers three aspects: (i) the volatility of the organo-sulfur compounds; (ii) the reactivity of the organo-sulfur compounds; (iii) the computation of non-reactive and reactive residue curve maps. The thermodynamic properties of the organo-sulfur compounds not reported in the literature are predicted through a group contribution method [23]. The basic design is validated through rigorous numerical simulations using ASPEN-PLUS.

2. The HDS reactive system and the element approach

In general, there are two possible reaction paths for sulfur removal from the organo-sulfur compounds, as illustrated for dibenzothiophene in Fig. 1. The first route is the sulfur atom direct extraction (hydrogenolysis) from the sulfured molecule. The second route is the hydrogenation of one aromatic ring followed by the sulfur atom extraction.

The dibenzothiophene (DBT) HDS reaction progresses preferentially via the direct extraction route [18]. When alkyl substituents are attached to the carbon atoms adjacent to the sulfur atom, the rate for direct sulfur extraction is diminished whereas the sulfur removal rate via the hydrogenation route is relatively unaffected. Co–Mo catalysts desulfurize primarily via the direct route, while the Ni-Mo catalyst do it via the hydrogenation route. The extent to which a given catalyst acts via one route or the other is determined by the H_2 and H_2S partial pressures and feed properties.

Despite 80% of the HDS of 4,6-DMDBT goes by the hydrogenation route with conventional sulfide Ni-Mo catalysts [20], due to the lack of thermodynamic data for this compound and the uncertainty on the predicted properties, the conceptual design is performed considering only DBT as the sulfur compound present in the diesel. Also, it is well known that HDS of DBT follows preferentially the direct extraction route [18] and in order to simplify the conceptual design, only this reaction route (hydrogenolysis) for DBT is considered. However, for its validation through numerical simulation, both, hydrogenolysis and hydrogenation routes are accounted. Modeling desulfurization kinetics of actual hydrocarbon streams is quite complex due to the presence of a wide variety of sulfur compounds, all of which have different reactivity. Therefore, for practical design purposes, desulfurization of various species may be lumped into the following

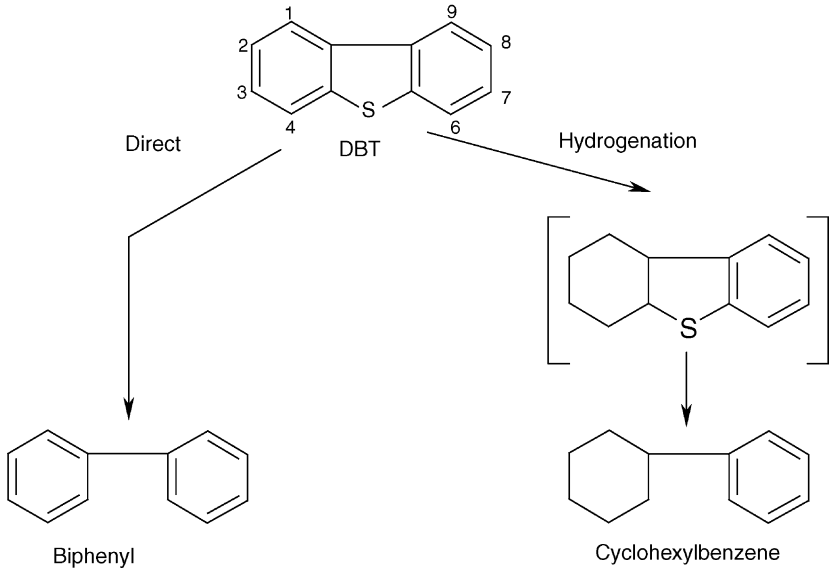

Fig. 1. Reaction pathways for HDS of DBT.

reaction:

$$v_1 \left\{ \begin{array}{l} \text{Th} \\ \text{BT} \\ \text{DBT} \\ \text{4, 6-DMDBT} \end{array} \right\} + v_2 H_2 \rightarrow v_3 \left\{ \begin{array}{l} \text{BD} \\ \text{Et} \\ \text{BPH} \\ \text{3-3}' \text{ DMBPH} \end{array} \right\} + v_4 H_2S \quad (1)$$

where Th represents thiophene; BT, benzothiophene; DBT, dibenzothiophene; 4,6-DMDBT, 4,6-dimethyl-dibenzothiophene; BD, butadiene; Et, ethylbenzene; BPH, biphenyl, 3-3′ DMBPH, 3-3′ dimethyl-biphenyl, and v_i are the appropriate stoichiometric coefficients. It can be noted that the hydrogenolysis reactions involve four species and they are carried out in a mixture of many hydrocarbons as solvent medium, i.e., a paraffinic blend of C_{10}–C_{16}. The computation and visualization of the phase behavior of this reactive mixture is difficult. This is because of the complexity of the reactive mixture containing H_2 and H_2S, and the lack of experimental values for thermodynamic properties of some organo-sulfur compounds, i.e., 4,6-dimethyl-dibenzothiophene and 3-3′ dimethyl-biphenyl. Assuming a reactive mixture with only *n*-C_{16} as solvent and using the element concept, a reduction of the composition space is possible. Thus, the above reactions can be written in terms of elements as:

$$v_1 AB + v_2 C + v_5 D \rightarrow v_3 A(v_2 - v_4)C + v_4 BC + v_5 D \quad (2)$$

where element A is the organic part of the sulfur compound, B the sulfur atom, C the hydrogen molecule and D is the inert solvent ($v_5 = 1$). The three-dimensional reactive space for DBT elimination is shown in Fig. 2. The shadowed areas correspond to the two-dimensional reactive zones. The general element matrix considering the four organo-sulfur compounds can be written as:

	Th, BT, DBT, 4,6-DMDBT (1)	H_2 (2)	BD, Et, BP, 3-3 DMBPH (3)	H_2S (4)	$C_{16}H_{34}$ (5)
A: Org	v_1	0	v_3	0	0
B: S	v_1	0	0	v_4	0
C: H_2	0	v_2	$v_2 - v_4$	v_4	0
D: $C_{16}H_{34}$	0	0	0	0	1

The element fractions (amount of element *j*/total amount of elements) are given as [26]:

$$W_A = \frac{v_1 x_1 + v_3 x_3}{2v_1 x_1 + v_2 x_2 + (v_3 + v_2 - v_4)x_3 + 2v_4 x_4 + x_5} \quad (3)$$

$$W_B = \frac{v_1 x_1 + v_4 x_4}{2v_1 x_1 + v_2 x_2 + (v_3 + v_2 - v_4)x_3 + 2v_4 x_4 + x_5} \quad (4)$$

$$W_C = \frac{v_2 x_2 + v_3 x_3 + (v_2 - v_4)x_3 + v_4 x_4}{2v_1 x_1 + v_2 x_2 + (v_3 + v_2 - v_4)x_3 + 2v_4 x_4 + x_5} \quad (5)$$

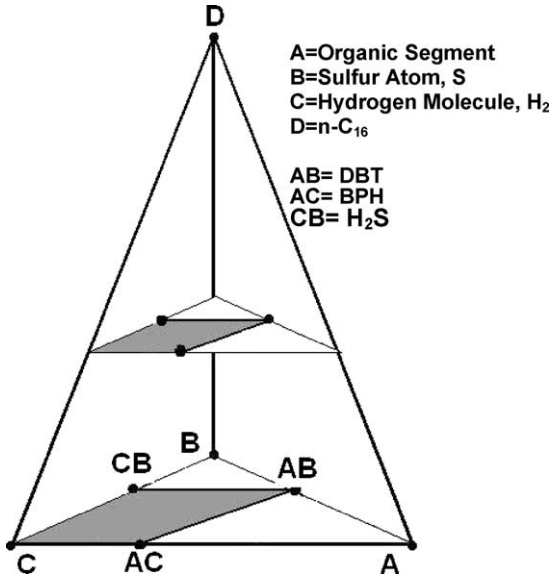

Fig. 2. Three-dimensional element composition space for hydrogenolysis of DBT.

$$W_D = \frac{x_5}{2v_1x_1 + v_2x_2 + (v_3 + v_2 - v_4)x_3 + 2v_4x_4 + x_5} \quad (6)$$

where x_i are the corresponding component mole fractions. Fig. 3 shows the normalized triangular phase diagram for the DBT hydrogenolysis reaction with or without solvent. It is obtained by setting $v_1 = 1$, $v_2 = 2$, $v_3 = 1$, $v_4 = 1$. With the above element fraction definition, the five species participating in the reaction are located in this reactive phase diagram. Also, if the solvent concentration is kept constant (W_D = constant), different normalized planes for the reactive mixture could be sketched (see upper plane in Fig. 2). The solvent free coordinates in the reactive diagram for the pure species are: DBT (0.5, 0.5, 0.0), H_2 (0, 0, 1), BPH (0.25, 0.0, 0.75), and H_2S (0.0, 0.5, 0.5).

3. Reactive residue curves map for hydrogenolysis of DBT

Considering only DBT as the sulfur-compound and $C_{16}H_{34}$ as the solvent, a reactive mixture of five species is obtained: DBT, H_2, BPH, H_2S and $C_{16}H_{34}$. The thermodynamic analysis considers, first of all, the computation of non-reactive residue curves. These curves are important in order to visualize the combined effect of the solvent concentration and the hydrogen and hydrogen sulfide solubility. The equations for computing the non-reactive residue curves are obtained by considering a batch distillation process and are written as:

$$\frac{dx_i}{dt} = \frac{\overline{V}}{H}(x_i - y_i) \quad (7)$$

where H is the molar liquid hold-up and $\overline{V}$ is the molar vapor flow rate. The quotient $H/\overline{V}$ is controlled via the heating input Q, and in this case the heating strategy is such that:

$$\frac{H}{\overline{V}} = \frac{H_0}{\overline{V}_0} = \text{constant} \quad (8)$$

This heating policy is physically significant and it leads to an autonomous model [41]. Substitution of Eq. (8) into Eq. (7) gives:

$$\frac{dx_i}{d\tau} = (x_i - y_i); \quad \text{with } d\tau = \frac{H_0}{\overline{V}_0}dt \quad (9)$$

The non-reactive residue curves for the reactive mixture considered are constructed by integration of Eq. (9) and they are shown in terms of element fractions in Fig. 4. The phase equilibrium calculations were performed using the Peng–Robinson [25] equation of state with the appropriate adjustable binary interaction coefficients used in the computation of the attractive parameter [3]. In order to avoid trivial solutions the phase stability test procedure proposed by Michelsen [24] was applied. The results obtained for the non-reactive residue curves at different solvent ($C_{16}H_{34}$) concentrations and P = 30 atm are shown in Fig. 4. The initial point for integration of Eq. (9) was

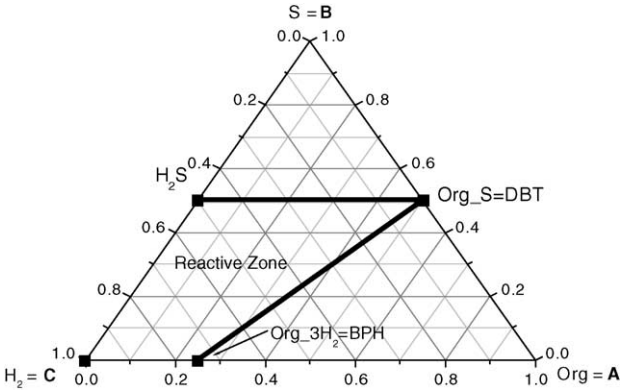

Fig. 3. Normalized triangular reactive composition diagram for hydrogenolysis of DBT for different solvent compositions (W_D = constant).

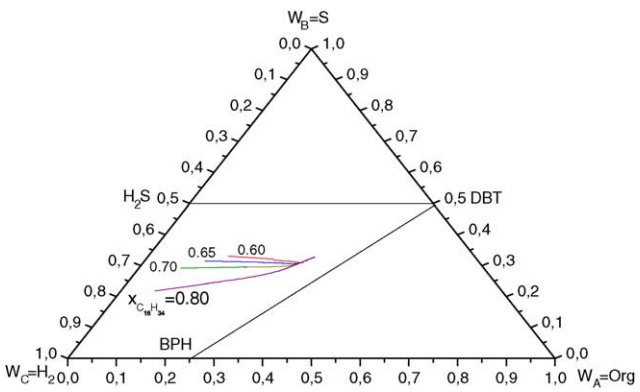

Fig. 4. Effect of the solvent concentration ($C_{16}H_{34}$) on the non-reactive residue curves for DBT reactive system.

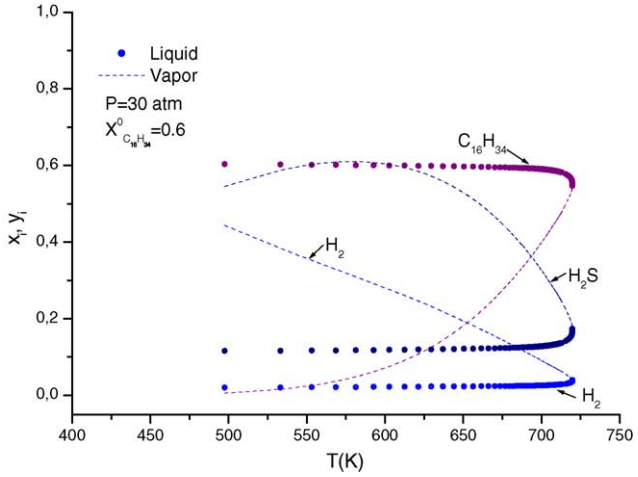

Fig. 5. Phase diagram (x–y–T) from the non-reactive residue curve for DBT reactive system with $x_{C_{16}H_{34}} = 0.6$.

$x^0_{DBT} = 0.110$, $x^0_{H_2} = 0.019$, $x^0_{BPH} = 0.110$, $x^0_{H_2S} = 0.101$, $x^0_{C_{16}H_{34}} = 0.660$, which corresponds to a boiling temperature of $T = 300$ K at $P = 30$ atm. Fig. 4 also shows that, if the solvent mole fraction increases from 0.6 to 0.8, the hydrogen solubility increases, as the element residue curve for the highest solvent composition is longer than the others. It should be noted that each residue curve corresponds to a different solvent concentration plane (see Fig. 2) and that the respective element fractions have been normalized to sum unity. The increase in hydrogen solubility can be noted in Figs. 5 and 6. Fig. 5 ($x_{C_{16}H_{34}} = 0.6$) shows that, for the entire temperature range, the hydrogen liquid mole fraction is close to a flat line, that is, constant solubility, and its value is below that for hydrogen sulfide. In contrast, Fig. 6 ($x_{C_{16}H_{34}} = 0.8$) exhibits a continuous increase in the hydrogen liquid composition until it equals the hydrogen sulfide solubility. Distinctively, in Fig. 6, for

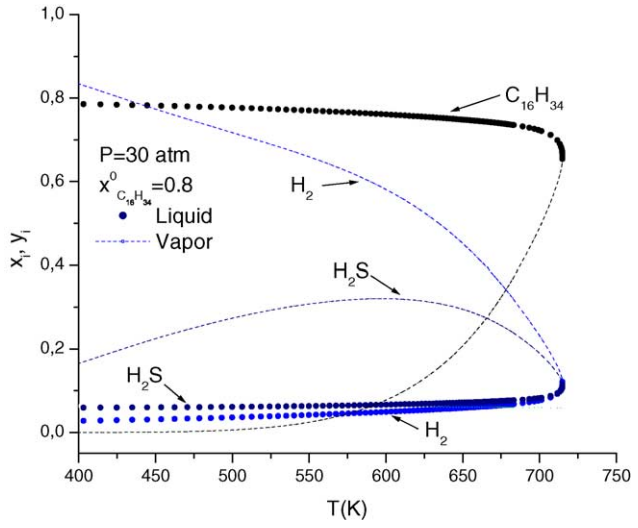

Fig. 6. Phase diagram (x–y–T) from the non-reactive residue curve for DBT reactive system with $x_{C_{16}H_{34}} = 0.8$.

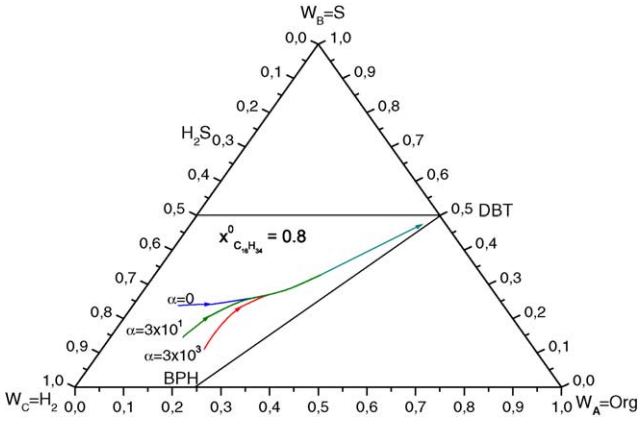

Fig. 7. Reactive residue curves for DBT reactive system with $C_{16}H_{34}$ as solvent; $P = 30$ atm.

the temperature range between 650 and 700 K, the hydrogen liquid mole fraction equals that of hydrogen sulfide. The visualization of the effect of the solvent concentration on the hydrogen solubility is an important result regarding the application of reactive distillation concepts. This, because the complete elimination of the heavier sulfur compounds requires high hydrogen concentration in the liquid phase [18].

The equations to compute the reactive residue curves are similar to those for the non-reactive case. However, the reaction term must be added into the mass balances. The *reactive* residue curves for hydrogenolysis of DBT with a solvent composition of $x_{C_{16}H_{34}} = 0.8$ are shown in Fig. 7. The reaction kinetic expression proposed by Broderick and Gates [7] has been used to compute such curves. The autonomous differential equations for computation of the reactive residue curves can be written as:

$$\frac{dx_i}{d\tau} = x_i - y_i + \alpha \sum_{j=1}^{NR} \left\{ \left[v_{ij} - \left(\sum_{k=1}^{NC} v_{kj} \right) x_i \right] \frac{r_j}{r_0} \right\} \qquad (10)$$

with the dimensionless reaction-separation parameter α given by:

$$\alpha = \frac{M_{cat} r_0}{\overline{V}_0} \qquad (11)$$

NC is the number of components participating in reaction j, NR is the number of reactions, M_{cat} is the catalyst mass (kg), $\overline{V}_0$ is the vaporization flow (kmol/h), r_j is the intrinsic rate of reaction j (kmol/(kg cat. h)), r_0 is a reference rate of reaction (1×10^{-4} kmol/(kg cat. h)) and v_{ij} is the stoichiometric coefficient of compound i in reaction j. The reaction-separation parameter α indicates the ratio between the amount of catalyst loaded in the distillation vessel (i.e., total wetted reacting area) multiplied by the reference rate of reaction to the vaporization flow. It should be noted that the parameter α has close resemblance to the Damkohler number, as it describes the conversion of a specific compound to its convective transport. However, in this case, it is preferred

to use the reaction-separation parameter to clearly indicate that a simultaneous reaction and separation phenomena is occurring. In fact, the reaction-separation parameter α indirectly accounts for a liquid residence time. It can be observed in Fig. 7 that, for values of $W_C \leq 0.5$ (low hydrogen concentrations), the reactive residues curves are similar to the non-reactive curve ($\alpha = 0$), and all curves point to a binary mixture of DBT and $x_{C_{16}H_{34}}$, as the hydrogen composition is reduced. This shows that, at boiling conditions, there is a critical hydrogen composition where the chemical reaction affects the phase split. If the amount of catalyst is augmented ($\alpha = 3 \times 10^1$) for $W_C > 0.5$, a separation of the reactive residue curves is noted. At higher values of α ($\alpha = 3 \times 10^3$), the reactive residue curve moves to the reactive boundary line limited by the BPH and DBT pure component nodes. Therefore, it is clear that, as the value of the reaction-separation parameter (α) increases, higher conversion to BPH is achieved. It should be pointed out that, a high value of α (i.e., $\alpha = 3 \times 10^3$) physically means high residence times, that is, large amounts of catalyst, and/or low vaporization flows (indicating the heating policy).

The effect of the chemical reaction on the component liquid compositions can be observed in Fig. 8. From 600 to 750 K, the liquid compositions of BPH and H_2S decrease and those of DBT and H_2 increase. The component liquid composition behavior may be explained as follows: at these thermodynamic conditions—600–750 K, $P = 30$ atm—the boiling process favors the vaporization of BPH and H_2S species, reducing their concentration in the liquid phase. Lowering the H_2S liquid concentration through vaporization is crucial, since this compound inhibits the desulfurization by the direct extraction route. It should be noted that the temperature range is close to the critical point of the reactive mixture. Therefore, despite the above convenient thermodynamic conditions, this high temperature region should be carefully considered for the design of a reactive section in a reactive distillation column.

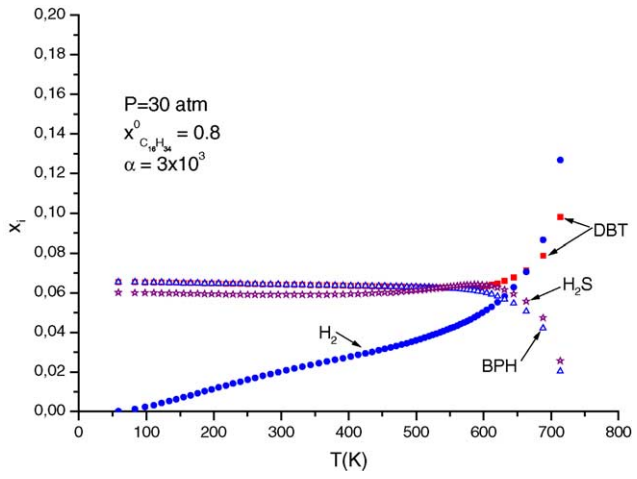

Fig. 8. Effect of the chemical reaction on the liquid composition for the reactive DBT system.

4. Conceptual design of a reactive distillation column for deep HDS

The conceptual design of the reactive distillation column for deep hydrodesulfurization of diesel is based on three aspects: (a) the volatility difference of the organo-sulfur compounds; (b) their different reactivities; (c) the analysis of the reactive residue curves.

4.1. Volatility of the organo-sulfur compounds

In order to apply the reactive distillation concepts, the knowledge of the reactive system vapor–liquid behavior is required. Compound volatilities or their normal boiling temperatures are the key thermodynamic properties, since they indicate the rate of vaporization/condensation of such compounds. The thermodynamic information for the heavier organo-sulfur compounds available in the open literature is rather scarce. From commercial sources (MERK, 2000) little information for 4,6-DMDBT is obtained. This lack of thermodynamic information leads to consider the prediction of the thermodynamic properties through group contribution methods or molecular simulation. In this work, the methods of Joback and Reid [17] and Marrero and Gani [23] were used. Table 2 shows some thermodynamic properties for the most representative organo-sulfur compounds obtained from commercial source (MERK, 2000) and those predicted with the group contribution methods. It may be observed that the normal boiling temperatures for Th and BTh are: 357 and 473.34 K, respectively, while for DBT is 587.98 and for 4,6-DMDBT 643.70 computed with Joback's method [17]. The difference in the normal boiling temperatures between BTh and DBT (≈115 K) indicates that it may be possible to group Th and BTh as the lighter organo-sulfur compounds and DBT and 4,6-DMDBT as the heavier ones. Therefore, due to the different volatilities, it may be expected that the lighter organo-sulfur compounds (Th and BTh) would concentrate in the rectifying section of a reactive distillation column and the heavier organo-sulfur compounds (DBT and 4,6-DMDBT) would concentrate in the stripping section.

4.2. Reactivity of the organo-sulfur compounds

The diesel organic sulfur compounds vary widely in their HDS reactivities. Deep HDS is not a simple conversion of total sulfur compounds by a pseudo first order reaction. The reactivities of the one- to three-ring sulfur compounds decrease in the order of thiophenes > benzothiophenes > dibenzothiophenes [11,14]. Gates and Topsoe [13] pointed out that 4-methyldibenzothiophene and 4,6-dimethyl-dibenzothiophene are the most appropriate compounds for investigations of candidate catalyst and reaction mechanisms, since they are among the most refractory sulfur species that remains in the diesel fuel after sulfur reduction to 500 wppm level by conventional hydrodesulfurization.

Table 2
Physical properties for some organo-sulfur compounds present in the diesel

	Commercial reference MERK (2000)	Joback–Reid [17]	Marrero–Gani [23]
Name	Thiophene		
CAS number	110-02-1		
Molecular formula	C4H4S		
Melting point (K)	235.2	234.45	234.02
Boiling point (K)	357.2	357.2	380.29
T_c (K)		579.31	590.21
P_c (bar)		57.13	58.37
Omega, ω		0.191	0.191
Name	1-Benzothiophene		
CAS number	95-15-8		
Molecular formula	C8H6S		
Melting point (K)	302.2–305.2	323.99	296.68
Boiling point (K)		473.34	508.20
T_c (K)		719.97	759.65
P_c (bar)		43.68	39.83
Omega, ω		0.332	0.350
Name	Dibenzothiophene		
CAS number	132-65-0		
Molecular formula	C12H8S		
Melting point (K)	370.2–372.2	415.05	382.04
Boiling point (K)	605.2–606.2	587.98	585.0
T_c (K)		853.65	882.92
P_c (bar)		37.59	44.51
Omega, ω		0.484	0.484
Name	4,6-Dimethyldi-benzothiophene		
CAS number	1207-12-1		
Molecular formula	C14H12S		
Melting point (K)	426.2–430.2	462.635	354.27
Boiling point (K)		643.70	601.05
T_c (K)		898.94	907.91
P_c (bar)		29.12	34.58
Omega, ω		0.584	0.584

Data from open literature and computed from two Group Contribution Methods, respectively.

Ma et al. [22] proposed to classify the sulfur compounds present in the diesel into four groups according to their HDS reactivities: (1) most of the alkyl BTs; (2) DBT and alkyl DBTs without substituents at the 4- and 6-positions; (3) alkyl DBTs with only one of substituents at either the 4- or 6-position; (4) alkyl DBTs with two of the alkyl substituents at the 4- and 6-positions, respectively. Based on this grouping, Sakanishi et al. [29,30] proposed a two-stage HDS conventional reactor using different catalyst for each stage, for deep HDS of diesel.

4.3. Analysis of the reactive residue curves

From the non-reactive and reactive residue curves, it is apparent that the elimination of DBT and 4,6-DMDBT may be favored at high temperatures (Fig. 8) and high solvent concentration (Fig. 4), whereas the elimination of Th and BT may be carried out at lower temperatures due to their lower volatilities. This leads directly to think a reactive distillation column consisting of two reactive zones: one zone of high temperature (stripping section) where preferential elimination of DBT and 4,6-DMDBT occurs with an appropriate catalyst, and another reactive zone (rectifying section) where Th and BT are eliminated at lower temperature. Fig. 9 shows a schematic diagram of such reactive distillation column. It should be clear that this reactive distillation column is thought to treat a partially desulfurized diesel (∼500 ppm of sulfur content). So that, the reactive distillation column should follow a conventional co-current trickle-bed single reactor. This conventional reactor-reactive distillation column configuration is different to the two-conventional reactors with an intermediate separator configuration described by Song and Ma [33].

5. Rigorous simulation of the reactive distillation column

After a basic conceptual design has been obtained, that is, a reactive distillation column comprising two reactive zones (considering non-reactive stages too), several column configurations were proposed and validated through numerical simulations [28]. It should be noted that, for the simulation of the reactive distillation column, an equilibrium model has

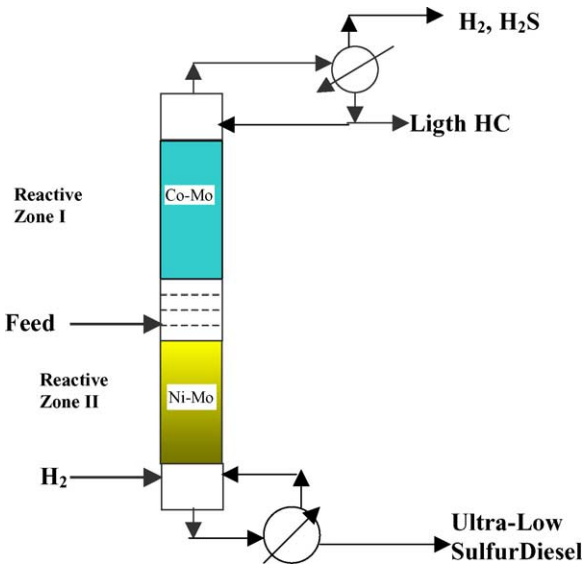

Fig. 9. Conceptual basic design of a reactive distillation column for ultra-low sulfur diesel production.

been assumed. That is, the heat and mass transport phenomena are not considered. The optimal column configuration consists of 15 stages, with 6 reactive stages. The reactive mixture modeling the sulfured-diesel fuel is a hydrocarbon mixture of C_{11}–C_{16} paraffin's with four organo-sulfur compounds: thiophene (Th), benzothiophene (BT), dibenzothiophene (DBT) and 4,6-dimethyl-dibenzothiophene (4,6-DMDBT). As first simulation case, the hydrocarbon mixture fed to the column has the following composition (mole fraction): $z_{Th} = 0.0087$, $z_{BT} = 0.0087$, $z_{DBT} = 0.1$, $z_{c11} = 0.4966$, $z_{c12} = 0.3166$, $z_{c13} = 0.0089$, $z_{c14} = 0.0015$, $z_{c16} = 0.0589$. It should be noted that the feed specifications are chosen to consider a diesel with 500 ppm of sulfur content. The operation pressure of the reactive column was set to 30 atm and a H_2/HC feed relation of 3 was used. Two kinetic expressions for the hydrogenolysis of DBT were used [7,10]. Table 3 shows the column configuration details for the simulations and Table 4 shows the design composition targets. It should be noted that in the first simulation case the 4,6-DMDBT compound is not considered in the feed stream and in a second simulation case, the concentration of 4,6-DMDBT was fixed to have 2.5% weight of sulfur compound content in the HC feed stream ($z_{Th} = 0.008$, $z_{BT} = 0.008$, $z_{DBT} = 0.1$, $z_{4,6\text{-DMDBT}} = 0.02$, $z_{c11} = 0.489$, $z_{c12} = 0.316$, $z_{c13} = 0.008$, $z_{c14} = 0.001$, $z_{c16} = 0.05$).

Table 3
Reactive distillation column configuration and design specifications

	Column specification
Reactive stages[a]	5–7, 10–12
Non-reactive stages	1–4, 8–9, 13–15
HC feed stage	9
H_2 feed stage	12
HC feed flow (kmol/h)	100
Distillate flow (kmol/h)	340
Reflux ratio	0.5
Top temperature (°C)	225
Column pressure (atm)	30
Hold-up (kg catalyst)	10000
Target conversion of DBT (case 1) (%)	99
Target conversion of 4,6-DMDBT (case 2) (%)	99
Th kinetic expression	Van Parijs and Froment [39]
BT kinetic expression	Van Parijs et al. [40]
DBT kinetic expression 1	Broderick and Gates [7]
DBT kinetic expression 2	Froment et al. [10]

[a] Stage 1 is a non-reactive partial condenser.

6. Results and discussion

The RDC rigorous steady state simulations were performed with ASPEN-PLUS. Fig. 10 shows the temperature profile along the reactive distillation column. It can be observed that reactive zone I operates close to isothermal, while in reactive zone II, the temperature raises around 15 degrees. The isothermal behavior of zone I is explained by observing

Table 4
Simulation results for the reactive distillation column design

Component	Feed (kmol/h) (case 1)	Feed (kmol/h) (case 2)	Bottom (kmol/h) (case 2) hydrogenolysis route	Bottom (kmol/h) (case 2) both routes
Th	0.87	0.8	1.2789E−16	0.0
BTh	0.87	0.8	3.865E−04	3.866E−04
DBT	10.0	10.0	4.605E−02	9.630E−03
4,6-DMDBT	0.0	2.0	6.468E−01	1.245E−02
$C_{11}H_{24}$	49.66	48.9	11.4685	11.2992
$C_{12}H_{26}$	31.66	31.6	16.1100	15.8935
$C_{13}H_{28}$	0.89	0.8	6.355E−08	6.307E−01
$C_{14}H_{30}$	0.15	0.1	9.445E−02	4.214E−02
$C_{16}H_{34}$	5.89	5.0	4.9820	4.9810
H_2	300 (at stage 12)	300	2.9071	2.8966
H_2S	0.0	0.0	6.225E−02	4.980E−02
BD	0.0	0.0	1.6033E−03	1.609E−03
Et	0.0	0.0	3.005E−02	2.969E−02
BPH	0.0	0.0	8.663	8.6417
DMBPH	0.0	0.0	0.6805	1.0838

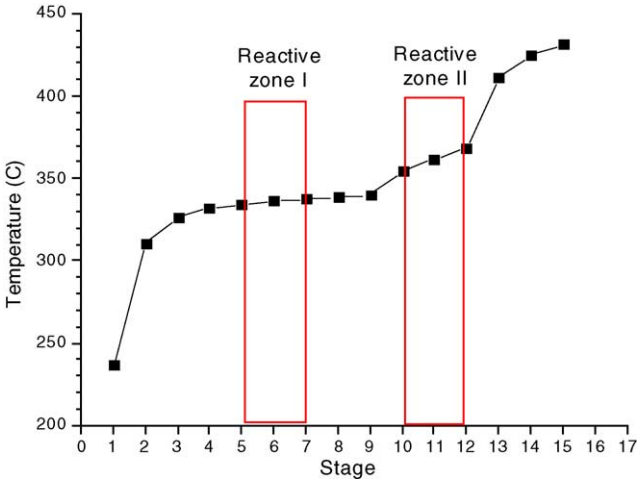

Fig. 10. Temperature profile along the reactive distillation column for deep HDS of diesel; kinetic expression 1.

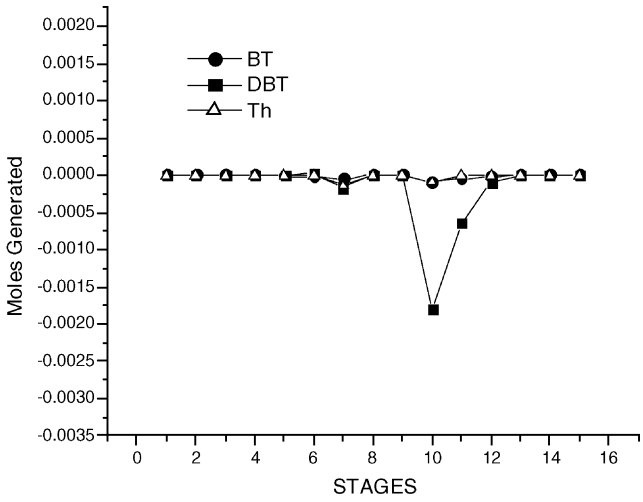

Fig. 12. Moles generated of Th, BT, and DBT along the reactive distillation column; kinetic expression 1.

two points: (i) the composition profile (see Fig. 11) shows that a mixture of C_{11} and C_{12} compounds is predominating in this zone leading to a boiling temperature for such mixture and (ii) the heat released by chemical reaction is negligible accordingly to the moles generated in this zone (see Fig. 12). On the other side, the temperature increment at zone II may be explained by noticing (Fig. 11) the concentration raise of the heavy hydrocarbons (i.e., *n*-hexadecane and BPH) and the moles generated (see Fig. 12) in this reactive zone.

The organo-sulfur compounds consumption in the two reactive zones considering only hydrogenolysis is shown in Fig. 12. The species are mainly consumed at stages 7 and 10, which are the incoming stages to the reactive zones. It should be pointed out that between the reactive zones there are two non-reactive stages (8 and 9) performing the separation and distribution of the organo-sulfur compounds. Fig. 13 shows the liquid composition profile of Th, BT and DBT along the column. It can be noted that the maximum compositions are located at the HC feed stage (stage 9). The highest concentration of DBT is due to the amount of DBT in the feed stream and its high boiling temperature. Also, it can be observed in Fig. 13 that as the organo-sulfur compounds go into the reactive zones (stages 5–7 and 10–12), the concentrations of the three species fall sharply to zero.

Fig. 14 shows the DBT liquid composition profile along the RDC using three different thermodynamic models. As was stated before, in order to obtain reliable results the appropriate binary interaction coefficients must be used in the equations of state. In this case, the binary coefficients were fixed to zero for SRK equation of state and the high DBT conversion achieved was similar to that with Peng–Robinson equation of state. However, when an activity coefficient model for the liquid phase is used (UNIQUAC), an unreliable behavior of the reactive system is obtained.

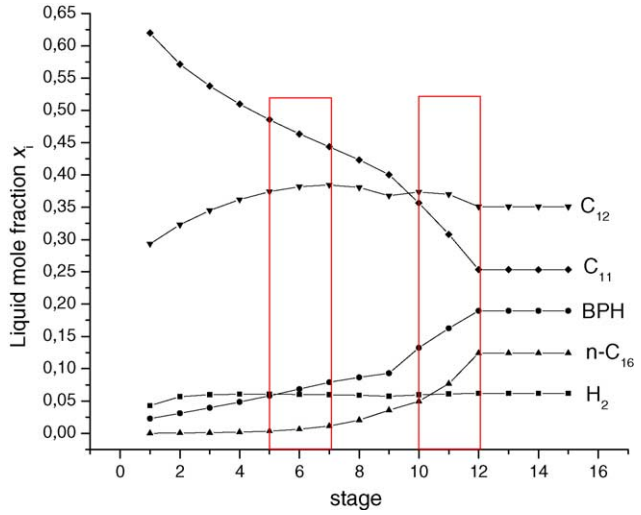

Fig. 11. Liquid composition profile along the reactive distillation column for H_2, C_{11}, C_{12}, BPH and *n*-C_{16}.

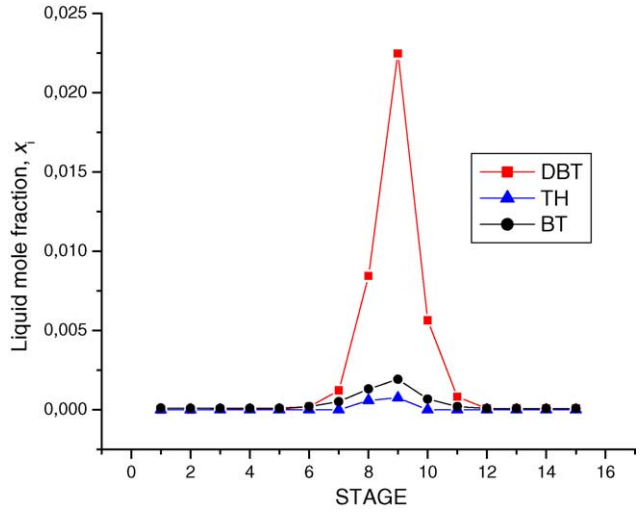

Fig. 13. Liquid composition profile for Th, BT, and DBT along the reactive distillation column; kinetic expression 1; hold-up: 1×10^3 kg of catalyst.

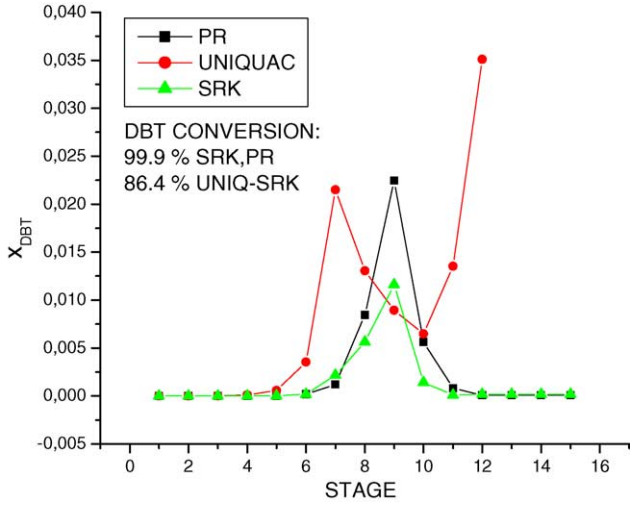

Fig. 14. Effect of the thermodynamic model on the DBT liquid composition profile.

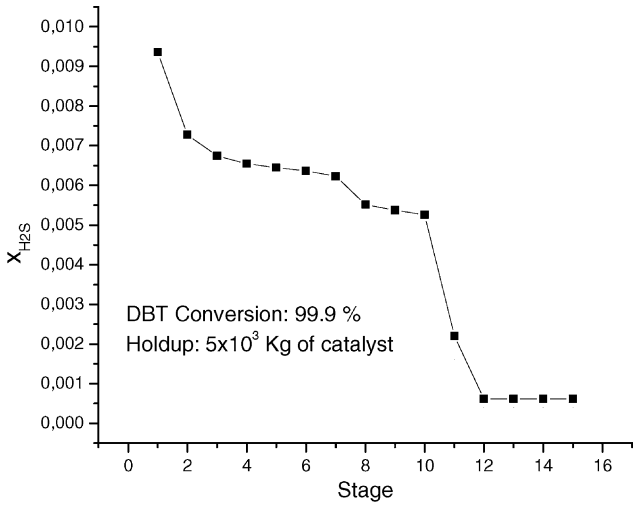

Fig. 16. H_2S liquid composition profile along the reactive distillation column; kinetic expression 1.

The effect of different rate of reaction expressions for the hydrogenolysis of DBT is shown in Fig. 15. There is almost no difference in the DBT conversion for the same amount of catalyst loaded in the reactive zones. However, for heavier sulfur-compounds (i.e., 4,6-DMDBT) it is highly recommendable to verify the kinetic expressions to be used in the simulations.

Fig. 16 shows the H_2S liquid composition along the RDC. The composition profile (higher concentration at the reactive zone I) suggests that the H_2S vaporization rate is larger at the stripping section. Therefore, the catalyst activity inhibition may be reduced at this section increasing the conversion of the heavier organo-sulfur compounds.

Figs. 17 and 18 show the RDC liquid composition profiles for DBT and 4,6-DMDBT for different number of reactive stages at the reactive zone II. The sharp reduction of the liquid concentration at reactive zone II is similar for both compounds and it is clear that, as the reactive stages increase, a full elimination of DBT is achieved. However, it can be observed in Fig. 18 that, while three reactive stages (15 total number of stages) at the stripping section are enough for complete elimination of DBT, two more reactive stages (17 total number of stages) are required to eliminate the 4,6-DMDBT.

Figs. 19 and 20 show the consumption profiles for the organo-sulfur compounds considering the hydrogenolysis and hydrogenolysis–hydrogenation routes, respectively. It can be noted, from Fig. 20, that the hydrogenation route increases substantially the consumption of DBT and 4,6-DMDBT. From the numerical results (see Table 4), it is observed that the conversion of 4,6-DMDBT increases from 67% to 99% when both reaction routes are considered. It is clear that for a realistic reactive distillation column design, the two reactions paths must be accounted.

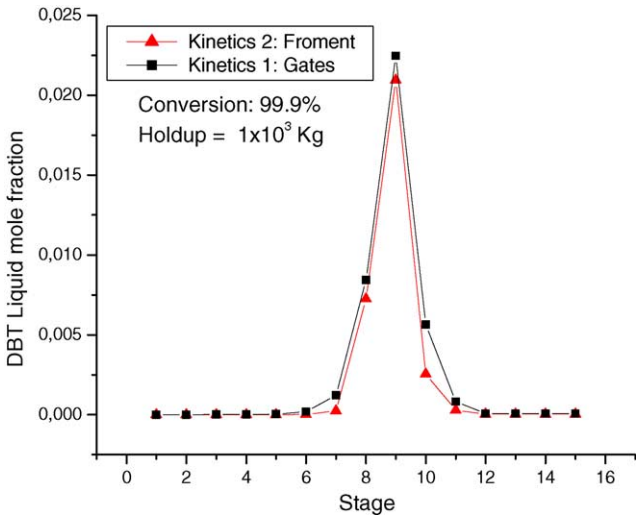

Fig. 15. Effect of the different reaction rate expressions on the DBT liquid composition profile.

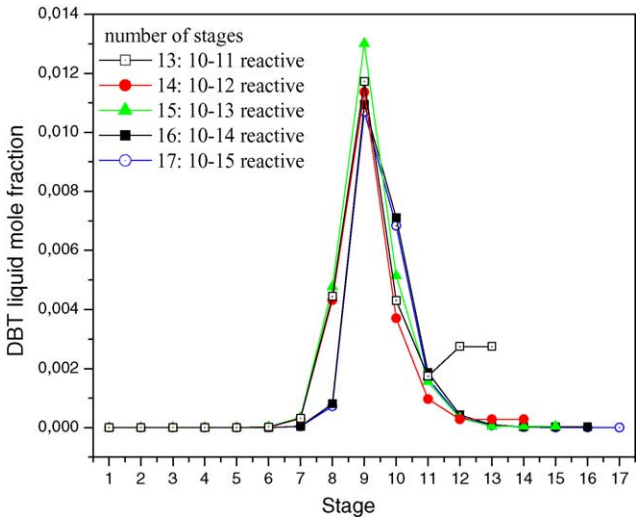

Fig. 17. Liquid composition profile of DBT along the reactive column for different number of reactive stages at stripping section; hold-up: 5×10^3 kg of catalyst.

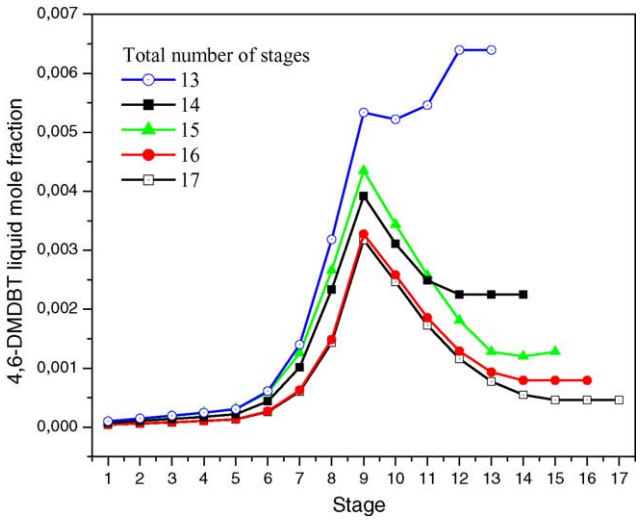

Fig. 18. Liquid composition profile of 4,6-DMDBT along the reactive column for different number of reactive stages at stripping section; hold-up: 5×10^3 kg of catalyst.

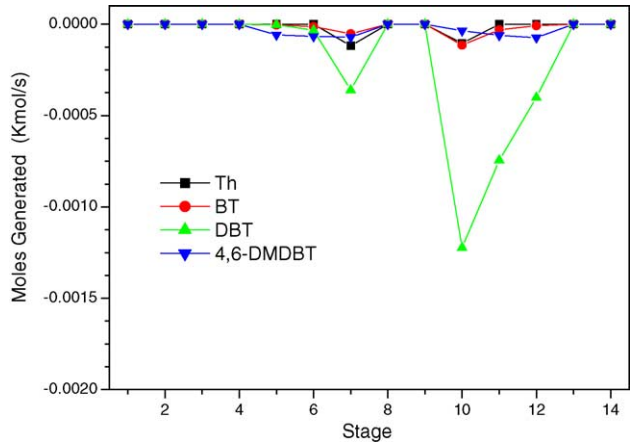

Fig. 19. Consumption profile for the organo-sulfur compounds considering only the hydrogenolysis reaction route; hold-up: 5×10^3 kg of catalyst.

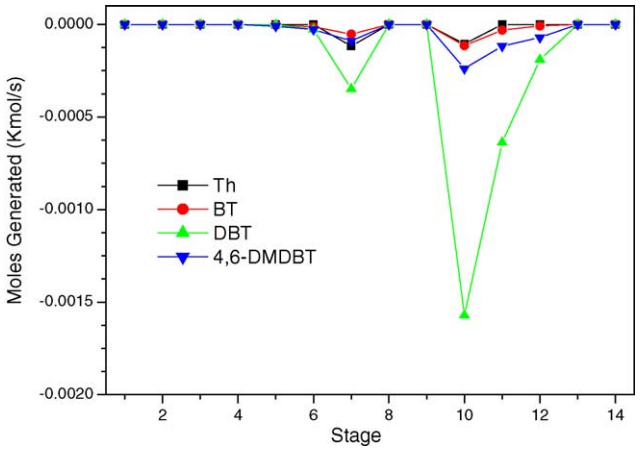

Fig. 20. Consumption profile for the organo-sulfur compounds considering (both) the hydrogenolysis and hydrogenation reaction routes; hold-up: 5×10^3 kg of catalyst.

7. Conclusions

Based on a thermodynamic analysis, the conceptual design of a reactive distillation column for deep HDS of diesel has been developed. The analysis is based on the computation of reactive and non-reactive residue curve maps for hydrogenolysis of DBT. It was found that the solvent concentration—or non-reactive hydrocarbon species (*n*-hexadecane)—is important in determining the solubility of hydrogen and hydrogen sulfide in the reactive mixture. The reactive residue curves show that there is a high temperature region where the vaporization process favors the elimination of DBT and 4,6-DMDBT.

The differences in volatility and reactivities of the organo-sulfur compounds, as well as the visualization of the residue curve trends, allow us for a conceptual design of a reactive distillation column consisting of two reactive zones. At the reactive zone I, located above the HC feed stream, Th and BT are preferentially eliminated, while DBT and 4,6-DMDBT are mainly consumed in reactive zone II. Rigorous steady state simulations showed that the presence of heavier organo-sulfur compounds (i.e., 4,6-DMDBT) do not affect the shape of the liquid concentration profiles along the reactive column, and the conceptual design obtained for DBT is still useful.

The analysis performed in this work and the simulation results shown that reactive distillation may be considered as a viable technological alternative for deep HDS of diesel. However, the uncertainty in physical properties and the associated phase behavior of the heavier sulfur-compounds and their respective HDS products suggest that much more experimental work should be done to verify the predicted data. Also, the operational aspects, such as stability and control of the reactive distillation column need to be considered.

Acknowledgement

The authors thank the financial support from CONACyT through the project U45160-Y.

References

[1] A.A. Abufares, P.L. Douglas, Mathematical modelling and simulation of an MTBE catalytic distillation process using SPEEDUP and ASPENPLUS, Trans. Ichem. Eng. 73A (1995) 3.
[2] V.H. Agreda, L.R. Partin, W.H. Heise, High-purity methyl acetate via reactive distillation, Chem. Eng. Prog. 86 (1990) 40.
[3] A. Anderko, Cubic and generalized Van der Waals equations, in: J.V. Sengers, R.F. Kayser, C.J. Peters, H.J. White Jr. (Eds.), Equations of State for Fluids and Fluid Mixtures. Part I., IUPAC Elsevier, 2000.
[4] http://www.itd.anl.gov/techtour/desulfur.html.
[5] D. Barbosa, M.F. Doherty, Design of multicomponent reactive distillation columns, Ichem. Eng. Symp. Series 194 (1988) B369.
[6] B. Bessling, G. Schembecker, K.H. Simmrock, Design of processes with reactive distillation line diagrams, Ind. Eng. Chem. Res. 36 (1997) 3032.

[7] D.H. Broderick, B.C. Gates, Hydrogenolysis and hydrogenation of dibenzothiophene catalyzed by sulfided CoO–MoO_3/γ-Al_2O_3: the reaction kinetics, AIChE J. 27 (4) (1981) 663.
[8] http://www.abb.se/.
[9] M.F. Doherty, G. Buzad, Reactive distillation by design, Trans. Inst. Chem. Engrs. 70A (1992) 448.
[10] G.F. Froment, G.A. Depauw, V. Vanrysselberghe, Kinetic modeling and reactor simulation in hydrodesulturization of oil fractions, Ind. Eng. Chem. Res. 33 (12) (1994) 2975.
[11] C.G. Frye, J.F. Mosby, Kinetics of hydrodesulfurization, Chem. Eng. Prog. 63 (1967) 66.
[12] E. Furimsky, Selection of catalyst and reactors for hydroprocessing, Appl. Catal. Gen. 171 (1988) 177–206.
[13] B.C. Gates, H. Topsoe, Reactivities in deep catalytic hydrodesulfurization: challenges, opportunities and the importance of 4-methyldibenzothiophene and 4,6-dimethyldibenzothiophene, Polyhedron 16 (1997) 3213.
[14] M.J. Girgis, B.C. Gates, Reactivities, Reaction networks and kinetics in high-pressure catalytic hydroprocessing, Ind. Eng. Chem. 30 (1991) 2021.
[15] R. Gonzalez, Optimize hydrotreating operations to produce more diesel, Hart's Fuel Technol. Manag. (1998).
[16] A. Hidalgo-Vivas, G.P. Towler, Distillate hydrotreatment by reactive distillation, in: Presented at AIChE Annual Meeting, November, 1998.
[17] K.G. Joback, R.C. Reid, Estimation of pure-component properties from group contribution, Chem. Eng. Commun. 57 (1987) 233–243.
[18] K.G. Knudsen, B.H. Cooper, H. Topsoe, Catalyst and process technologies for ultra low sulfur diesel, Appl. Catal. Gen. 189 (1999) 205–215.
[19] R. Krishna, Reactive separations: more ways to skin a cat, Chem. Eng. Sci. 57 (2002) 1491–1504.
[20] J.M. Manoli, P. Da Costa, M. Brun, M. Vrinat, F. Maugé, C. Potvin, Hydrodesulfurization of 4,6-dimethylbenzothiophene over promoted (Ni, P) alumina-supported molybdenum carbide catalysts: activity and characterization of active sites, J. Catal. 221 (2004) 365–377.
[21] R. Monroy, E.S. Pérez-Cisneros, J. Alvarez, A robust PI control configuration for a high-purity ethylene glycol reactive distillation column, Chem. Eng. Sci. 55 (2000) 4925.
[22] X. Ma, K. Sakanishi, I. Mochida, Hydrodesulfurization reactivities of various compounds in diesel fuel, Ind. Eng. Chem. Res. 33 (1994) 218–222.
[23] J. Marrero, R. Gani, Group–contribution based estimation of pure component properties, Fluid Phase Equilib. 183–184 (2001) 183–208.
[24] M.L. Michelsen, The isothermal flash problem. Part I. Stability, Fluid Phase Equilib. 9 (1982) 1–19.
[25] D.Y. Peng, D.B. Robinson, A new two constant equation of state, Ind. Eng. Chem. Fundam. 15 (1976) 59–64.
[26] E.S. Pérez-Cisneros, R. Gani, M.L. Michelsen, Reactive separation systems. Part I. Computation of physical and chemical equilibrium, Chem. Eng. Sci. 52 (1997) 527.
[27] E.S. Pérez-Cisneros, Modelling, design and analysis of reactive separation process, Ph.D. Thesis, Technical University of Denmark, 1997.
[28] E.S. Perez-Cisneros, S.A. Granados-Aguilar, P. Huitzil-Melendez, T. Viveros-Garcia, Design of a reactive distillation process for ultra-low sulfur diesel production, in: Proceedings of ESCAPE-12, vol. 10, 2002, pp. 301–306.
[29] K. Sakanishi, M. Ando, S. Abe, I. Mochida, Extensive desulfurization of diesel fuel through catalytic two-stage hydrotreatment, J. Jpn. Pet. Inst. 34 (1991) 553.
[30] K. Sakanishi, M. Ando, S. Abe, I. Mochida, Extensive desulfurization of diesel fuel through catalytic two-stage hydrotreatment. Part 2. Influence of reaction pressure on desulfurization and reactivities of refractory sulfur compounds, J. Jpn. Pet. Inst. 35 (1992) 403.
[31] O. Sánchez-Daza, E. Bek-Pedersen, E.S. Pérez-Cisneros, R. Gani, Graphical and stage-to-stage methods for reactive distillation column design, AIChE J. 49 (11) (2003) 2822–2841.
[32] L.A. Smith, M.N. Huddleston, New MTBE design now commercial, Hydrocarbon Process. 3 (1982) 121.
[33] C. Song, X. Ma, New design approaches to ultra-clean diesel fuels by deep desulfurization and deep dearomatization, Appl. Catal. B Environ. 41 (2003) 207–238.
[34] R. Taylor, R. Krishna, Modeling reactive distillation, Chem. Eng. Sci. 55 (2000) 5183–5229.
[35] C. Thiel, K. Sundmacher, U. Hoffmann, Synthesis of ETBE: residue curve maps for heterogeneously catalyzed reactive distillation process, Chem. Eng. J. 66 (1997) 181–191.
[36] H. Topsoe, F.E. Massoth, B.S. Clausen, Hydrotreating catalyst, in: J.R. Anderson, M. Boudart (Eds.), Catalyst Science and Technology, vol. 11, Springer Berlag, Berlin, 1996.
[37] S. Ung, M.F. Doherty, Vapour–liquid phase equilibrium in system with multiple chemical reactions, Chem. Eng. Sci. 50 (1995) 23.
[38] B.W. Van Hasselt, P.J.M. Lebens, H.P.A. Calis, F. Kapteijn, S.T. Sie, J.A. Moulijn, C.M. van den Bleek, A numerical comparison of alternative three-phase reactors with a conventional trickle-bed reactor. The advantages of countercurrent flow for hydrodesulfurization, Chem. Eng. Sci. 54 (1999) 4791–4799.
[39] I.A. Van Parijs, G.A. Froment, Kinetics of hydrodesulfurizations on a CoMo/γAl_2O_3 catalyst. Part 1. Kinetics of the hydrogenolysis of thiophene, Ind. Eng. Chem. Prod. Res. Dev. 25 (1986) 431.
[40] I.A. Van Parijs, L.H. Hosten, G.F. Froment, Kinetics of hydrodesulfurization on a CoMo/γAl_2O_3 catalyst. Part 2. Kinetics of hydrogenolysis of benzothiophene, Ind. Eng. Chem. Prod. Res. Dev. 25 (1986) 437.
[41] G. Venimadhavan, G. Buzad, M.F. Doherty, M.F. Malone, Effect of kinetics on residue curve maps for reactive distillation, AIChE J. 40 (11) (1994) 1814–1824.